Lin et al. Nanoscale Research Letters (2015) 10:74
DOI 10.1186/s11671-015-0791-9

Nanoscale Research Letters
a SpringerOpen Journal

NANO EXPRESS Open Access

A facile approach to prepare silicon-based Pt-Ag tubular dendritic nano-forests (tDNFs) for solar-light-enhanced methanol oxidation reaction

Chun-Ting Lin[1,2*], Ming-Hua Shiao[1], Mao-Nan Chang[3,4], Nancy Chu[1], Yu-Wei Chen[3], Yu-Hsuan Peng[2], Bo-Huei Liao[1], Hung Ji Huang[1], Chien-Nan Hsiao[1] and Fan-Gang Tseng[2,5*]

Abstract

In this paper, a facile two-step Galvanic replacement reaction (GRR) is proposed to prepare Pt-Ag tubular dendritic nano-forests (tDNFs) in ambient condition for enhancing methanol oxidation reaction (MOR) under solar illumination. In the first GRR, a homogeneous layer of silver dendritic nano-forests (DNFs) with 10 μm in thickness was grown on Si wafer in 5 min in silver nitride ($AgNO_3$) and buffer oxide etchant (BOE) solution. In the second GRR, we utilized chloroplatinic acid (H_2PtCl_6) as the precursor for platinum (Pt) deposition to further transform the prepared Ag DNFs into Pt-Ag tDNFs. The catalytic performance and solar response of the Pt-Ag tDNFs toward methanol electro-oxidation are also studied by cyclic voltammetry (CV) and chronoamperometry (CA). The methanol oxidation current was boosted by 6.4% under solar illumination on the Pt-Ag tDNFs due to the induced localized surface plasmon resonance (LSPR) on the dendritic structure. Current results provide a cost-effective and facile approach to prepare solar-driven metallic electrodes potentially applicable to photo-electro-chemical fuel cells.

Keywords: Direct methanol fuel cell; Galvanic replacement reaction; Tubular dendritic nano-forests

Background

Direct methanol fuel cell (DMFC) has been deemed as one of the important power suppliers for renewable power applications due to the high energy-conversion efficiency thereof [1,2]. One of the major issues of DMFCs is the slow process of methanol oxidation reaction (MOR), which directly limits the efficiency of DMFC [3]. Traditionally, platinum (Pt)-based alloy has been used as common a catalyst in MOR. In the past two decades, many bimetallic catalysts have been proposed to enhance the efficiency of MOR, including Pt-Ru [4], Pt-Ag [5], Pt-Au [6], etc. Recently, metal-oxide-supported Pt catalysts, including Pt-TiO_2 [7], Pt-ZnO [8], and PtRu-TiO_2 [9], were proposed to boost methanol oxidation under ultraviolet (UV) illumination for photo-electrochemical fuel cells [9]. Although over 60% of enhancement on MOR has been realized under UV illumination (365 nm, 100 W) [8], seldom, reports discussed the solar enhancement toward MOR, especially on pure metallic catalysts. In this paper, a facile two-step Galvanic replacement reaction (GRR) is proposed to prepare Pt-Ag tubular dendritic nano-forests (tDNFs) in ambient condition for enhancing MOR under solar illumination.

In preparation of the aforementioned bimetallic catalysts, GRR was widely employed to provide a simple and cost-effective fabrication approach [10,11]. By utilizing the difference in the standard reduction potentials, replacement between two metals can be easily achieved at ambient condition. Many metal composites prepared by GRR have been reported, including Ag-Au [12,13], Pt-Au [14,15], Pd-Pt [16,17], Ag-Pt [18-21], Pd-Ag [22,23], Cu-Pd [24], and Cu-Ag [25]. However, most of the studies focused on the preparation of non-supported catalysts.

* Correspondence: chunting@narlabs.org.tw; fangang@ess.nthu.edu.tw
[1]Instrument Technology Research Center, National Applied Research Laboratories, Hsinchu 300, Taiwan
[2]Department of Engineering and System Science, National Tsing Hua University, Hsinchu 300, Taiwan
Full list of author information is available at the end of the article

The prepared catalysts suspended in the solution could be hardly collected and deposited on the electrodes in the electrochemical cells. Moreover, the effective electrochemical surface area of the non-supported catalysts could be greatly sacrificed due to the aggregation of nano-catalysts in brushing or printing process [4,26].

In order to prepare metallic nanostructures directly on supporting substrates, fluoride-assisted Galvanic replacement reaction (FAGRR) was proposed to synthesize three-dimensional metallic dendrites on silicon-based substrates [27-31]. Recently, Ye et al. reported a facile method for preparing self-assembled silver dendrites on silicon wafer in fluoride and silver nitride solution [27,29] for improving surface-enhanced Raman spectroscopy (SERS) [27-29,31]. However, the prepared silver dendrites could be easily contaminated by sulfur or oxygen to from Ag_2O or Ag_2S at ambient [32,33], which directly limits the applications for catalytic reactions.

In this paper, we propose the preparation of Si-based Pt-Ag tDNFs for solar-light-enhanced MOR by a two-step facile GRR at ambient without any energy input. This self-assembled Pt-Ag tDNFs not only benefit from the large aspect surface area provided by the Ag dendrites but also the localized surface plasmon resonance (LSPR) effect for the enhancement of methanol electrode-oxidation. Besides, the Pt outer shell of Pt-Ag tDNFs provides a protection to Ag and thus greatly enhances the stability of the prepared photo-electrodes.

Methods

Preparation of Ag DNFs and Pt-Ag tDNFs

A two-step-GRR is proposed to prepare the Si-based Pt-Ag tDNFs as shown in Figure 1. In the first step of GRR, a fluoride-assisted GRR (FAGRR) [30] was adopted to prepare the Ag dendritic nanoforests (Ag DNFs) on planar silicon. In a typical process, n-type silicon (2 cm × 2 cm) was dipped into 2.5 mM silver nitride ($AgNO_3$) + 25% (v/v) buffered oxide etchant (BOE) (comprising 34% NH_4F and 7% HF) for 5 min at ambient. Following this, the sample underwent DI wash and N_2 spray, and the Ag DNFs are ready as a scaffold for the next process. In the second step of GRR, the Si-based Ag DNFs were immersed into a 0.5 mM chloroplatinic acid (H_2PtCl_6) electrolyte for 5 min in ambient atmosphere for Pt deposition. The prepared samples were then immersed in 30% NH_4OH for 1 h to remove AgCl precipitate [34]. After DI wash and dehydration bake at 105°C for another 5 min, the Pt-Ag tDNFs were ready for experiment. We also prepared a sample by sputtering 7 nm of Pt on one-step GRR-prepared Ag DNFs, which is denoted as S-Pt/Ag DNFs, for comparison.

Surface morphology and material characterization

Scanning electron microscope (SEM; Hitachi FE 4300 in Instrument Technology Research Center (ITRC); Hitachi, Tokyo, Japan) and field emission transmission electron microscope (TEM; JOEL JEM2100F in National Chung Hsing University (NCHU); JOEL Ltd., Tokyo, Japan) were employed to investigate the surface profile of the prepared samples. Energy-dispersive X-ray spectroscopy (EDS) was used to analyze the elemental composition.

Investigation on photo-enhanced electrochemical reactions

Electrochemical reactions were measured by a potentiostat (Autolab PGSTAT302N in ITRC) in a rectangular three-electrode reaction tank (500 mL) made by quartz. The prepared samples with projection area of 1 cm^2 were used as the working electrodes, Pt-coated titanium mesh (25 cm^2) as the counter electrode, and saturated calomel electrode (SCE) as the reference electrode. Cyclic voltammetry (CV) and chronoamperometry (CA) were used to evaluate the catalytic capability for methanol electro-oxidation. A solar simulator (SADHUDESIGN; class B; 400 to 1,000 nm; 1,000 W m^{-2}) was employed for the illumination experiments. All chemicals used in this experiment were reagent grade. The resistance of DI water was 18.2 MΩ. All experiments were conducted at 22°C at ambient pressure.

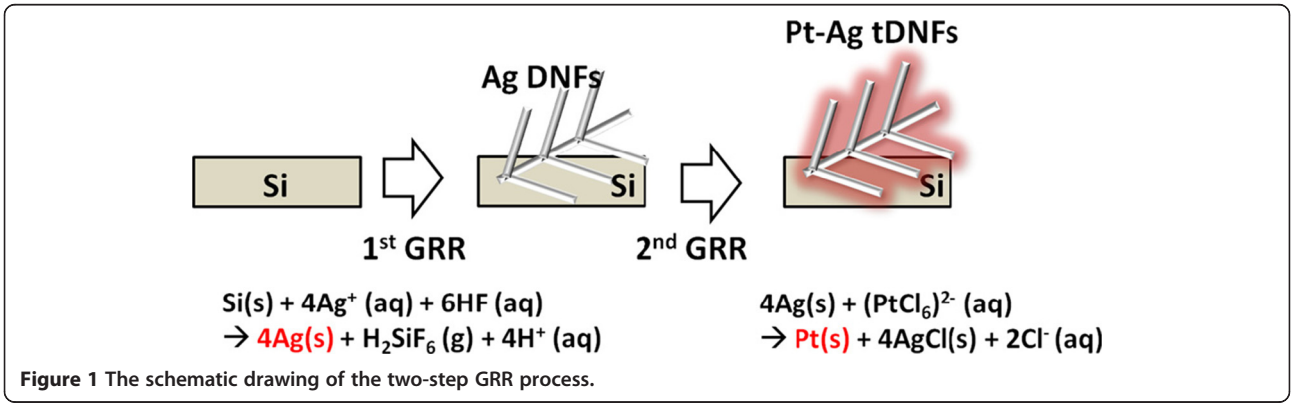

Figure 1 The schematic drawing of the two-step GRR process.

Results and discussion

Surface morphology of Ag DNFs

The SEM images shown from Figure 2a,b,c,d demonstrate the typical Ag DNFs on silicon substrate obtained by the first GRR. A 10-μm-thick Ag DNF layer was homogeneously formed on a plain silicon substrate within 5 min. It is found that oxygen signal was not detected in the as-prepared Ag DNFs in the EDS analysis (Figure 2e). This indicates our process is not favored for the formation of silver oxide. The growing process of Ag DNFs is schematically depicted in Figure 3. In the early stage of the reaction, Ag nano-islands dominated the surface of Si (Figure 3a). The dendritic structures started to appear after 40 s of the FAGRR and finally extended to the whole surface of Si (Figure 3b,c,d,e,f). The cross-section views (Figure 3g,h,i) demonstrate that the thickness of the Ag DNFs layer could reach 10 μm in 5 min and 20 μm in 8 min, respectively, which has not been reported in the previous studies on silicon-based silver dendrites [27-29]. The 10-μm-thick Ag DNFs (Figure 3i) were selected for the following experiments.

Surface morphology of Pt-Ag tDNFs

Figure 4 shows the SEM investigations of typical Pt-Ag tDNFs and the corresponding EDS analysis result. The morphology of the Pt-Ag DNFs basically follows that of the Ag DNFs while the branches were broadened. The composition of Pt was verified by the EDS analysis (Figure 4d). Figure 5 shows the TEM and scanning transmission electron microscope (STEM) images of the Pt-Ag tDNFs. Dark nano-shells (approximately 20 nm in thickness) were found growing along with the fringe of Ag branches in the bright field images (Figure 5a,c,d,e). The nano-shells were found bright in the high-angle annular dark-field (HAADF) images in Figure 5b. Since HAADF images are highly sensitive to atomic-number contrast [35], we hence verified that a thin layer of Pt nano-shell was grown over the whole surface of Ag branches. The tubular nature of Pt-Ag tDNFs was verified by the EDS linear scan in Figure 5f. The main reason of the formation of the hollow structures could be attributed to the difference in diffusion rate between Ag in Pt and Pt in Ag during the GRR process, which is known as the Kirkendell effect [10]. Since the diffusion rate of Ag in Pt is faster than that of Pt in Ag, the voids in Ag domain accumulated to form pores beneath the outer shell and finally occupied the cores of the dendrites [10,21,36]. Besides, several parallel dark lines were observed growing along with the long axis of the composite dendrite in the Ag core region in Figure 5d,e. That provides an evidence to the Kirkendall growth of Pt, which is the main mechanism of the formation of multi-layered metallic nanostructures in GRR [36]. Similarly, hollow Pt-Ag hybrid structures prepared via GRR were also reported by other groups [19-21]. Zhang et al. used GRR to fabricate Pt/Ag hollow nanoboxes for methanol oxidation [19]. Bansal et al. replaced Ag nanocubes with Pt by GRR for H_2 evolution reaction [20]. Also, Kim et al. prepared hollow Pt/Ag nanospheres by GRR for the degradation of rhodamine B [21].

Photo-enhancement on methanol electro-oxidation

Figure 6 shows the cyclic voltammograms (CVs) of various working electrodes in 0.5 M NaOH + 1 M CH_3OH. Both S-Pt/Ag DNFs and Pt-Ag tDNFs showed activity toward methanol electro-oxidation. The peak current densities of MOR of S-Pt/Ag DNFs and Pt-Ag DNFs are located at 1.65 and 6.10 mA cm^{-2}, respectively. Also, it is found that Ag DNFs showed no activity toward methanol electro-oxidation. Only typical redox couple of Ag is observed in the CVs of the Ag DNFs, which coincides with the previous reports [5,37]. Figure 7 shows

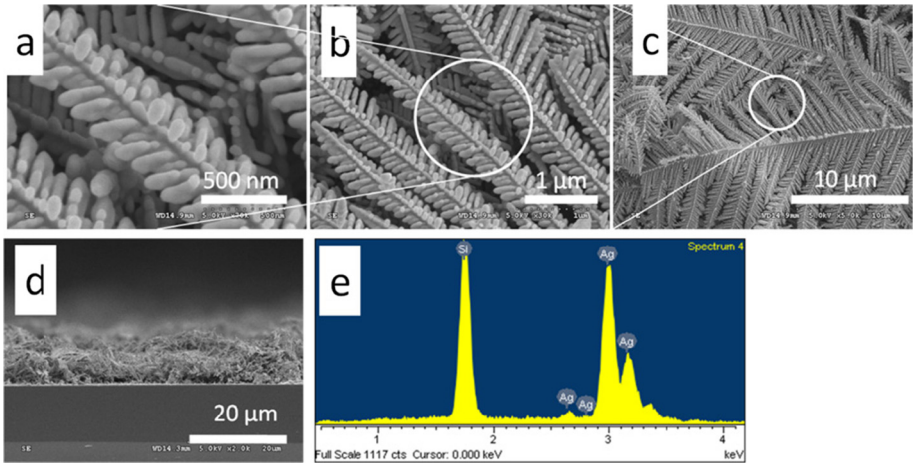

Figure 2 The SEM images and EDS result of Ag DNFs. (a-d) The SEM images of typical Ag DNFs grown on plane silicon in 2.5 mM $AgNO_3$ and 25% (*v/v*) buffered oxide etchant (BOE) for 300 s. **(e)** The EDS result of the Ag DNFs shown in **(a)**.

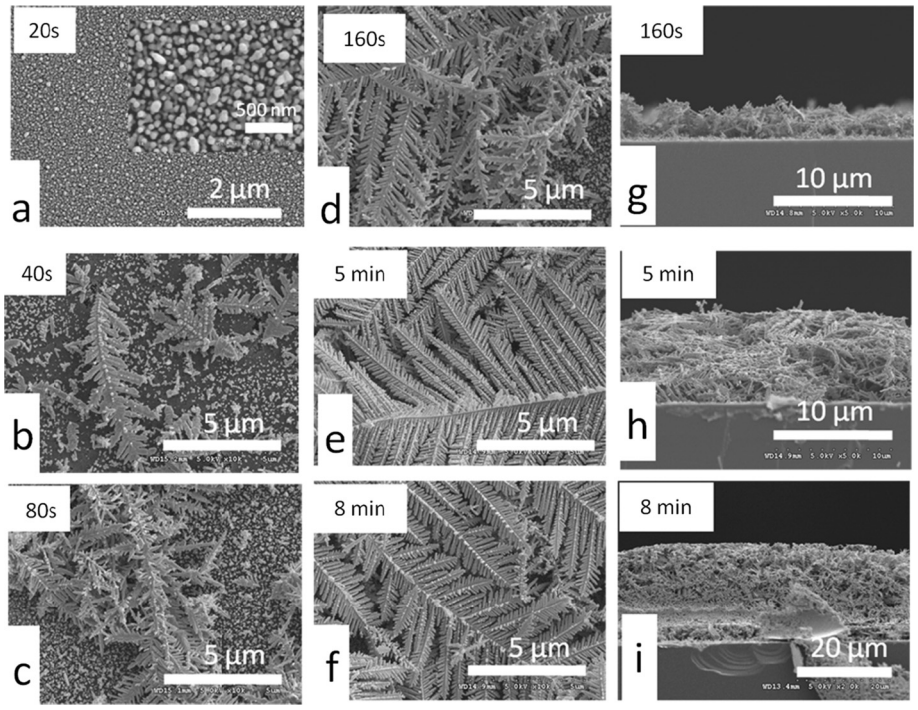

Figure 3 The top (a-f) and side view (g-i) of SEM images of Si-based Ag nano-islands and Ag DNFs for various reaction durations.

the on-off tests in CA with −0.3 V_{SCE} of bias applied to various working electrodes. All of the samples showed solar enhancement for MOR. In the first illumination cycle, the oxidation currents were boosted from 4.81 to 5.12 mA (6.4% of enhancement) and from 4.11×10^{-4} to 4.31×10^{-4} A (4.87% of enhancement) for Pt-Ag tDNFs and S-Pt/Ag DNFs, respectively (Figure 7b,c). Moreover, pulses of oxidation current were detected on Ag DNFs under illumination. In the first illumination cycle on the Ag DNFs, the oxidation current jumped from -5.14×10^{-5} to 4.10×10^{-5} A and was followed by a sharp decay to negative current region again within 2 s (Figure 7d). In the Ag DNFs, the strong electric field generated by LSPR results in the hot spots on specific confined areas of the

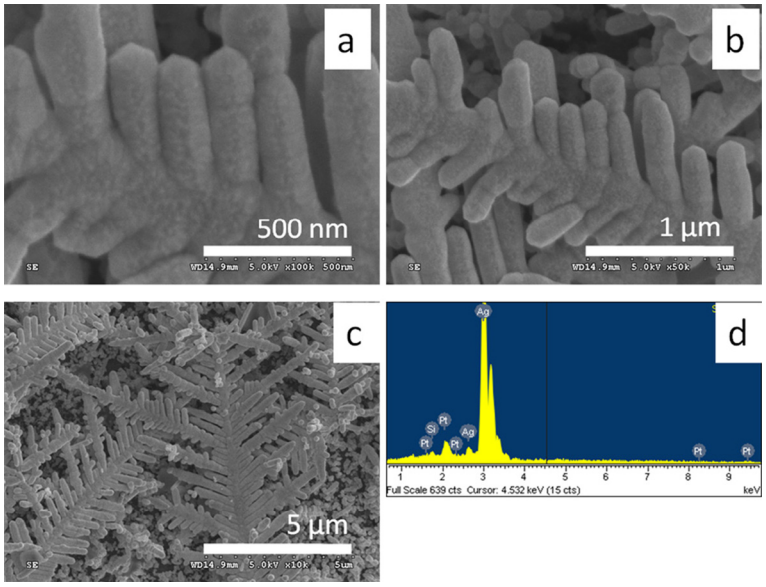

Figure 4 The SEM images and EDS result of typical Pt-Ag tDNFs. (a-c) The SEM images of typical Pt-Ag tDNFs. **(d)** The corresponding EDS result.

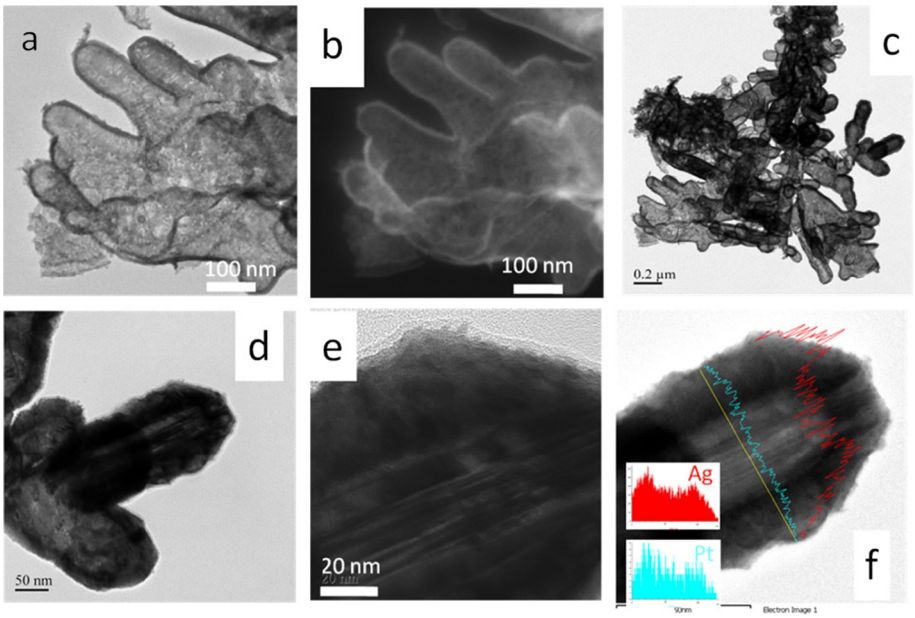

Figure 5 STEM bright-field image, high-angle annular dark-field STEM image, TEM images, and EDS result. (a) The STEM bright-field image of typical Pt-Ag tDNFs. **(b)** The high-angle annular dark-field (HAADF) STEM image of the same sample. **(c-e)** The TEM images in different magnifications of the same sample. **(f)** The corresponding EDS linear result.

dendritic structures. That helps deprive electrons from the adjacent methanol molecules and contribute to methanol electro-oxidation [38-40]. The sharp decay of oxidation current also suggests that only very limited methanol molecules in the hot spot region involved in the electron transfer process. In the cases of S-Pt/Ag DNFs and Pt-Ag tDNFs, the LSPR boosted the catalytic capability of Pt in the hot spot region and directly contributed to the oxidation current in the MOR. Also, more stable cyclic performance on photo-enhancement was found on Pt-Ag tDNFs when compared to that of S-Pt/Ag DNFs. That suggested the GRR provides better interface quality between Pt and Ag in Pt-Ag tDNFs.

Figure 8 shows the open-circuit potential (OCP) variation under identical cyclic illumination performed in Figure 7. Negative shifts of OCP were found on all of the samples under illumination. The OCP variations at

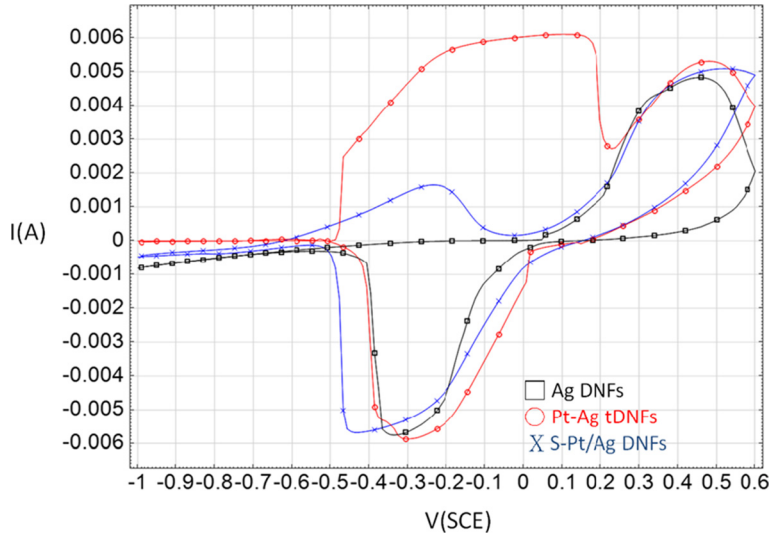

Figure 6 Cyclic voltammograms of various working electrodes in 1 M CH_3OH + 0.5 M NaOH at 22°C in ambient condition. Counter electrode: Pt-coated Ti mesh; reference electrode: saturated calomel electrode (SCE); scan rate = 30 mV/s.

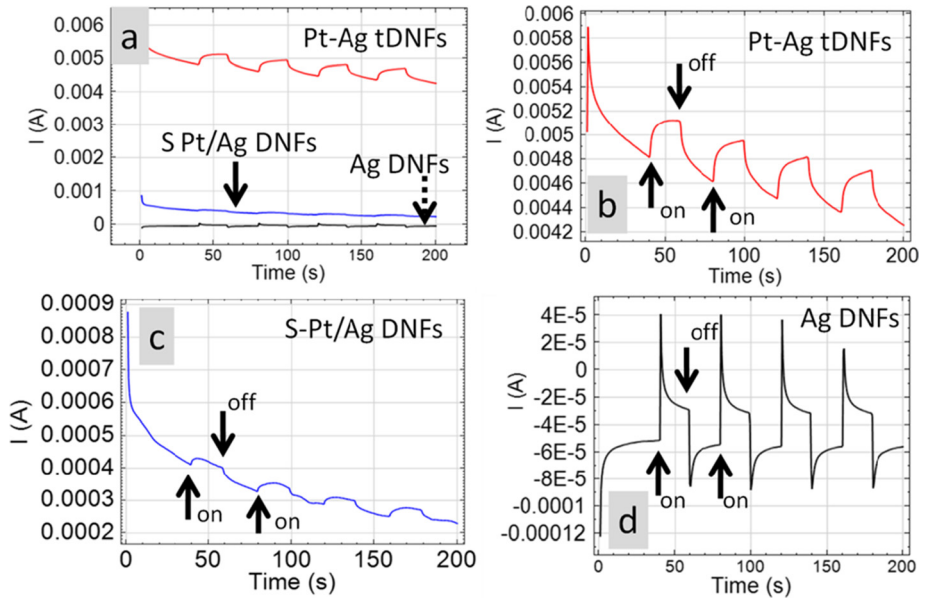

Figure 7 The chronoamperometric (CA) on-off test of various working electrodes. (a) The CA plots of various working electrodes. **(b-d)** The enlarged CA plots from **(a)** for Pt-Ag tDNFs, S-Pt/Ag DNFs, and Ag DNFs, respectively. The polarization potential is −0.3 V_{SCE}. Counter electrode: Pt-coated Ti mesh; reference electrode: saturated calomel electrode (SCE). The illumination was conducted under a solar simulator (SADHUDE-SIGN; class B; 400 to 1,000 nm; 1,000 W m^{-2}).

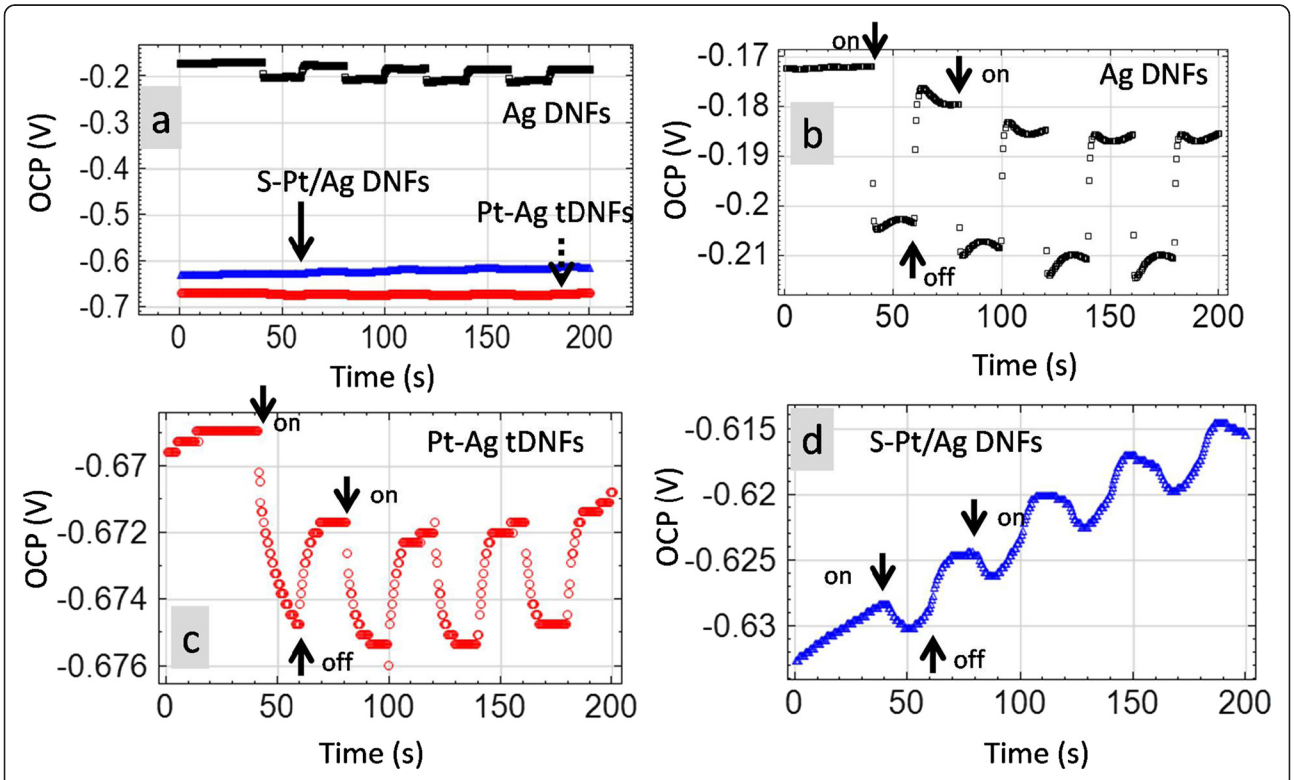

Figure 8 The open-circuit potential (OCP) of various working electrodes during the on-off test under illumination. (a) The OCP plots of various working electrodes. **(b-d)** The enlarged OCP plots from **(a)** for Ag DNFs, Pt-Ag tDNFs, and S-Pt/Ag DNFs, respectively. Counter electrode: Pt-coated Ti mesh; reference electrode: saturated calomel electrode (SCE). The illumination was conducted under a solar simulator (SADHUDE-SIGN; class B; 400 to 1,000 nm; 1,000 W m^{-2}).

the first cycle of illumination were −0.06 V (−0.9%), −0.002 V (−0.3%), and −0.03 V (−19.2%) for Pt-Ag tDNFs, S-Pt/Ag DNFs and Ag DNFs, respectively. The trend of OCP variation coincides with that of the current enhancement. This negative shift in OCP could be explained as the change in the electronic state of the working electrodes, i.e., Pt-Ag DNFs, S-Pt/Ag DNFs, and Ag DNFs. Since Ag DNFs are well known as effective SERS substrates [27,41], we herein believe the strong LSPR effect played a crucial rule in the catalytic process [42]. Meanwhile, the Pt-Ag tDNFs show better cyclic stability than the S-Pt/Ag DNFs in OCP on-off measurement. That coincides with the results found in CA on-off test.

The mechanism of LSPR enhancement on electrocatalysis is a synergetic process, comprising plasmonic heating, magnification of local electromagnetic field, electron injection process, etc. [40-43]. Although more experiments are required to further elucidate the energy transfer process, current results provided a direct observation on the oxidation current enhancement and OCP variation under solar illumination in methanol electrooxidation. The cost-effective and easily-prepared silicon-based Pt-Ag tDNFs are active to solar illumination and have high potential to serve as promising candidates for photo-electrochemical fuel cells.

Conclusions

In this letter, focus is placed on the facile two-step GRR to prepare silicon-based Pt-Ag tDNFs in ambient condition for enhancing MOR under solar illumination. The FAGRR enables the fast growth of Ag NDFs on the silicon wafer within 5 min. Following that, the chloroplatinic acid further transformed the surface of Ag NDFs into Pt nano-shells and emptied the structure simultaneously within another 5 min. The prepared Pt-Ag tDNFs showed solar response (6.4% of enhancement on oxidation current) toward methanol oxidation. The solar response is attributed to the strong LSPR provided by the Ag DNFs. This cost-effective Pt-Ag tDNFs could be a promising candidate for photo-electrochemical fuel cells.

Competing interests

The authors declare that they have no competing interests.

Authors' contributions

CT and FG conceived the research work and prepared the manuscript jointly. FG is the principal investigator of this research project. MH, MN, BH, and CN participated in the major discussion and contributed to the interpretation of the surface analytical results. HJ participated in the major discussion and contributed to the interpretation of photochemical mechanism. NC contributed to the SEM investigation. YW and YH contributed to the preparation of experimental samples. All authors read and approved the final manuscript.

Acknowledgements

The authors would like to express appreciation to the Ministry of Science and Technology of the Republic of China, Taiwan, for the financial supports under the following contract numbers: MOST103-2321-B-007-004, NSC102-2321-B-007-006, MOST103-3113-E-007-006, NSC102-2627-M-007-002, MOST104-2623-E-492-001-ET, and NSC102-2221-E-492-003. Also, we appreciate Mr. Chih-Jung Lu at the Instrument Center in National Chung Hsing University for his help in TEM operation.

Author details

[1]Instrument Technology Research Center, National Applied Research Laboratories, Hsinchu 300, Taiwan. [2]Department of Engineering and System Science, National Tsing Hua University, Hsinchu 300, Taiwan. [3]Department of Physics, National Chung Hsing University, Taichung 402, Taiwan. [4]Institute of Nanoscience, National Chung Hsing University, Taichung 402, Taiwan. [5]Division of Mechanics, Research Center for Applied Sciences, Academia Sinica, Taipei 115, Taiwan.

Received: 28 November 2014 Accepted: 30 January 2015
Published online: 18 February 2015

References

1. Li X, Faghri A. Review and advances of direct methanol fuel cells (DMFCs) part I: design, fabrication, and testing with high concentration methanol solutions. J Power Sources. 2013;226:223–40.
2. Olah GA. Beyond oil and gas: the methanol economy. Angew Chem Int Ed. 2005;44:2636–9.
3. Liu H, Song C, Zhang L, Zhang J, Wang H, Wilkinson DP. A review of anode catalysis in the direct methanol fuel cell. J Power Sources. 2006;155:95–110.
4. Tsai M-C, Yeh T-K, Tsai C-H. An improved electrodeposition technique for preparing platinum and platinum-ruthenium nanoparticles on carbon nanotubes directly grown on carbon cloth for methanol oxidation. Electrochem Commun. 2006;8:1445–52.
5. Feng Y-Y, Bi L-X, Liu Z-H, Kong D-S, Yu Z-Y. Significantly enhanced electrocatalytic activity for methanol electro-oxidation on Ag oxide-promoted PtAg/C catalysts in alkaline electrolyte. J Catal. 2012;290:18–25.
6. Zeng J, Yang J, Lee JY, Zhou W. Preparation of carbon-supported core-shell Au-Pt nanoparticles for methanol oxidation reaction: the promotional effect of the Au core. J Phys Chem B. 2006;110:24606–11.
7. Lin C-T, Huang HJ, Yang J-J, Shiao M-H. A simple fabrication process of Pt-TiO2 hybrid electrode for photo-assisted methanol fuel cells. Microelectronic Engineering. In Press, Accepted Manuscript.
8. Su C-Y, Hsueh Y-C, Kei C-C, Lin C-T, Perng T-P. Fabrication of high-activity hybrid Pt@ZnO catalyst on carbon cloth by atomic layer deposition for photoassisted electro-oxidation of methanol. J Phys Chem C. 2013;117:11610–8.
9. Drew K, Girishkumar G, Vinodgopal K, Kamat PV. Boosting fuel cell performance with a semiconductor photocatalyst: TiO2/Pt-Ru hybrid catalyst for methanol oxidation. J Phys Chem B. 2005;109:11851–7.
10. Xia X, Wang Y, Ruditskiy A, Xia Y. 25th anniversary article: galvanic replacement: a simple and versatile route to hollow nanostructures with tunable and well-controlled properties. Adv Mater. 2013;25:6313–33.
11. Carraro C, Maboudian R, Magagnin L. Metallization and nanostructuring of semiconductor surfaces by galvanic displacement processes. Surf Sci Rep. 2007;62:499–525.
12. Au L, Lu X, Xia Y. A comparative study of galvanic replacement reactions involving Ag nanocubes and AuCl2− or AuCl4−. Adv Mater. 2008;20:2517–22.
13. Yang L, Qi M, Jin M. Fabrication of SBA-15 supported Ag@Au-Ag metal-core/alloy-shell nanoparticles for CO oxidation. CrystEngComm. 2013;15:2804–8.
14. Chen L, Kuai L, Yu X, Li W, Geng B. Advanced catalytic performance of Au–Pt double-walled nanotubes and their fabrication through galvanic replacement reaction. Chem Eur J. 2013;19:11753–8.
15. Kim Y, Kim HJ, Kim YS, Choi SM, Seo MH, Kim WB. Shape- and composition-sensitive activity of Pt and PtAu catalysts for formic acid electrooxidation. J Phys Chem C. 2012;116:18093–100.
16. Zhang H, Jin M, Wang J, Li W, Camargo PHC, Kim MJ, et al. Synthesis of Pd–Pt bimetallic nanocrystals with a concave structure through a bromide-induced galvanic replacement reaction. J Am Chem Soc. 2011;133:6078–89.
17. Wang L, Yamauchi Y. Metallic nanocages: synthesis of bimetallic Pt–Pd hollow nanoparticles with dendritic shells by selective chemical etching. J Am Chem Soc. 2013;135:16762–5.
18. He W, Wu X, Liu J, Zhang K, Chu W, Feng L, et al. Formation of AgPt alloy nanoislands via chemical etching with tunable optical and catalytic properties. Langmuir. 2009;26:4443–8.

19. Zhang W, Yang J, Lu X. Tailoring galvanic replacement reaction for the preparation of Pt/Ag bimetallic hollow nanostructures with controlled number of voids. ACS Nano. 2012;6:7397–405.
20. Bansal V, O'Mullane AP, Bhargava SK. Galvanic replacement mediated synthesis of hollow Pt nanocatalysts: significance of residual Ag for the H2 evolution reaction. Electrochem Commun. 2009;11:1639–42.
21. Kim MR, Lee DK, Jang D-J. Facile fabrication of hollow Pt/Ag nanocomposites having enhanced catalytic properties. Appl Catal B Environ. 2011;103:253–60.
22. Huang J, Vongehr S, Tang S, Lu H, Meng X. Highly catalytic Pd–Ag bimetallic dendrites. J Phys Chem C. 2010;114:15005–10.
23. Liu M, Lu Y, Chen W. PdAg nanorings supported on graphene nanosheets: highly methanol-tolerant cathode electrocatalyst for alkaline fuel cells. Adv Funct Mater. 2013;23:1289–96.
24. Mohl M, Dobo D, Kukovecz A, Konya Z, Kordas K, Wei J, et al. Formation of CuPd and CuPt bimetallic nanotubes by galvanic replacement reaction. J Phys Chem C. 2011;115:9403–9.
25. Chen X, Cui C-H, Guo Z, Liu J-H, Huang X-J, Yu S-H. Unique heterogeneous silver–copper dendrites with a trace amount of uniformly distributed elemental Cu and their enhanced SERS properties. Small. 2011;7:858–63.
26. Lin C-T, Huang HJ, Yang J-J, Shiao M-H. A simple fabrication process of Pt-TiO2 hybrid electrode for photo-assisted methanol fuel cells. Microelectron Eng. 2011;88:2644–6.
27. Ye W, Shen C, Tian J, Wang C, Bao L, Gao H. Self-assembled synthesis of SERS-active silver dendrites and photoluminescence properties of a thin porous silicon layer. Electrochem Commun. 2008;10:625–9.
28. Fei Chan Y, Xing Zhang C, Long Wu Z, Mei Zhao D, Wang W, Jun Xu H, et al. Ag dendritic nanostructures as ultrastable substrates for surface-enhanced Raman scattering. Appl Phys Lett. 2013;102:183118-183118-183115.
29. Ye W, Shen C, Tian J, Wang C, Hui C, Gao H. Controllable growth of silver nanostructures by a simple replacement reaction and their SERS studies. Solid State Sci. 2009;11:1088–93.
30. Lin C-T, Yu M-H, Su J, Chen P-L, Shiao M-H, Nemcsics A, et al. Localized electroless Ag plating at a tip apex for scanning Kelvin probe microscopy. Jpn J Appl Phys. 2013;52:06GF03-06GF03-04.
31. Gutés A, Carraro C, Maboudian R. Silver dendrites from galvanic displacement on commercial aluminum foil as an effective SERS substrate. J Am Chem Soc. 2010;132:1476–7.
32. Saber TMH, El Warraky AA. AES and XPS study on the tarnishing of silver in alkaline sulphide solutions. J Mater Sci. 1988;23:1496–501.
33. McMahon MD, Lopez R, Meyer III HM, Feldman LC, Haglund Jr RF. Rapid tarnishing of silver nanoparticles in ambient laboratory air. Appl Phys B. 2005;80:915–21.
34. Chen HM, Liu R-S, Asakura K, Lee J-F, Jang L-Y, Hu S-F. Fabrication of nanorattles with passive shell. J Phys Chem B. 2006;110:19162–7.
35. Otten MT. High-angle annular dark-field imaging on a tem/stem system. Journal of Electron Microscopy Technique. 1991;17:221–30.
36. Gonzalez E, Arbiol J, Puntes VF. Carving at the nanoscale: sequential galvanic exchange and kirkendall growth at room temperature. Science. 2011;334:1377–80.
37. Shim JH, Yang J, Kim S-j, Lee C, Lee Y. One dimensional Ag/Au/AgCl nanocomposites stemmed from Ag nanowires for electrocatalysis of oxygen reduction. J Mater Chem. 2012;22:15285–90.
38. Han X, Wang D, Huang J, Liu D, You T. Ultrafast growth of dendritic gold nanostructures and their applications in methanol electro-oxidation and surface-enhanced Raman scattering. J Colloid Interface Sci. 2011;354:577–84.
39. Huang X, Tang S, Mu X, Dai Y, Chen G, Zhou Z, et al. Freestanding palladium nanosheets with plasmonic and catalytic properties. Nat Nano. 2011;6:28–32.
40. Adleman JR, Boyd DA, Goodwin DG, Psaltis D. Heterogenous catalysis mediated by plasmon heating. Nano Lett. 2009;9:4417–23.
41. Fei Chan Y, Xing Zhang C, Long Wu Z, Mei Zhao D, Wang W, Jun Xu H, et al. Ag dendritic nanostructures as ultrastable substrates for surface-enhanced Raman scattering. Applied Physics Letters 2013;102:183118–183118-5.
42. Kale MJ, Avanesian T, Christopher P. Direct photocatalysis by plasmonic nanostructures. ACS Catal. 2013;4:116–28.
43. Hou W, Cronin SB. A review of surface plasmon resonance-enhanced photocatalysis. Adv Funct Mater. 2013;23:1612–9.